Hindawi
Mobile Information Systems
Volume 2022, Article ID 2916971, 7 pages
https://doi.org/10.1155/2022/2916971

Research Article

Three-Dimensional Dynamic Visualization Simulation of Underground Mining Engineering considering Chaos Optimization of Symmetric Varieties

Guozhi Lu, Rui Wang, Qianshun Li, and Fei Hu

College of Energy and Mining Engineering, Shandong University of Science and Technology, Qingdao 266590, China

Correspondence should be addressed to Rui Wang; lgz2050@sdust.edu.cn

Received 10 May 2022; Accepted 28 June 2022; Published 31 July 2022

Academic Editor: Muhammad Muzammal

Aiming at the complex situation of mine underground engineering, this paper is chaos optimization to design 3D visualization simulation system of mine underground engineering, especially to satisfy the basic functions of 3D dynamic system and chaos optimization algorithm. A symmetric manifold algorithm is adopted. Explanations, transformation methods, and projective transformation methods and optical processing and conventional vector calculation techniques are used for analyzing underground mining engineering cases; it can be seen as follows: chaos-optimized symmetric variety algorithms in real life as an example. It can offer new ideas for optimizing the composition of underground mining engineering.

1. Introduction

The 3D dynamic visualization system of downhole mine engineering is rather complicated. As the production at mines and factories continue to change [1, 2], the overall balance, engineering continuity, uncertainty, and randomness at different links should be considered in 3D dynamic visual simulation of downhole mine engineering [3, 4] for its effective recognition, optimization, and dynamic visual simulation. With the rapid progress of science and technology, digitization and visualization technology have been extensively applied in many fields. The plan for developing the mine engineering simulation system is prepared, digitized, and visualized, the changes in the mine pit engineering are recorded and expressed timely and accurately, and the management level and work efficiency of the mine is enhanced.

Nowadays, domestic research and development institutions have designed simulation systems for downhole mining engineering. This system is of great significance to computer-aided mining design and planning. However, it is invalid in the 3D visual simulation of engineering construction. Visualization techniques such as light, material, and texture mapping can effectively display the complexity and dynamics of the 3D spatial relationship of downhole mine engineering.

2. Chaos Optimization Symmetric Manifold Algorithm and Application

2.1. Chaos Optimization Symmetric Manifold Algorithm. Chaos is a common nonlinear phenomenon with complex and random behavior [5, 6], which, however, is regular to some extent. The concept of chaos is a game-changer to the progress of science. Chaos has the following unique features: susceptibility of the initial value, cruising, and self-generating characteristics can be used to optimize the mechanism, thereby avoiding falling into the minimum in the process of exploration. Chaotic variables are used to optimize symmetrical manifolds, which is better than random symmetrical manifolds. Hence, chaos is a new optimization technology, which has received widespread attention, and has been researched deeply by scholars at home and abroad.

There are two main methods for chaotic optimization of symmetric manifolds. The idea is basically the same. Considering the traversal trajectory generated by the chaotic

optimization symmetric manifold iteratively, when certain optimization conditions are met, problems can be found in the symmetric manifold. This point serves as the symmetrical manifold at the start of the next step; the secondary carrier method searches through chaotic changes in a small interval of traversal nearby; the space is continuously reduced based on the variable-metric method for generating new solutions and generating disturbances near the temporary "optimum" point.

Chaos optimization algorithm is chosen to optimize, where chaos optimization is generated by Logistic model, and search for optimization in this paper.

$$x_{(n+1)} = \lambda x_n (1 - x_n). \tag{1}$$

In the formula, $\lambda = 4$. If n parameters need to be optimized, n different initial values are set arbitrarily in the interval (0, 1) (note that it cannot be the nondynamic point 0.25, 0.5, 0.75 of equation (1)) to maximize the different chaos of n trajectories, which are converted into chaotic variables in the optimization of the problem solution space, and the optimal solution of the problem is obtained through search.

It is often tricky to identify the optimal solution for multi-function optimization issues. In most cases, each target is adjusted in a balanced manner as the case may be to obtain the optimal balanced solution with certain precision and practical significance [7, 8]. The decisive objective function and constraints are described, and the chaotic optimization issue is solved by intelligent algorithm based on the fuzzy theory. The dark color for over 1,000 targets is applicable to the optimal dextrin of basic single targets. In the fuzzy set of optimal solutions, the solution to each target is obtained if possible.

(1) The objective function for MOP issue is complicated, and only a huge membership function is provided. The maximum is the prerequisite to comply with the constraints. Higher goals are preferred, and the upper limit (no lower one) is set. The upper limit is the optimal value for optimizing each goal. Hence, correlation function takes the shape of ray for each target, as shown below.

$$\mu(f_k(X)) = \begin{cases} 1, & f_k(X) > c_{01}, \\ \dfrac{f_k(X) - c_{0k} + \delta_{0k}}{\delta_{0k}}, & c_{0k} - \delta_{0k} < f_k(X) \le x_{0k}, \\ 0, & f_k(X) \le c_{0k} - \delta_{0k}, \end{cases} \tag{2}$$

where $\mu(f_k(X))$ is the membership function for target $f_k(X)$ (Figure 1); c_{0k} is the optimized value of single-objective target $f_k(X)$; δ_{0k} is the value added by target $f_k(X)$ acceptable to the decision-maker, which is determined according to the value of the single-objective optimized target after a certain degree of expansion and contraction.

The specific steps for solving the chaotic optimization symmetric manifold are described below:

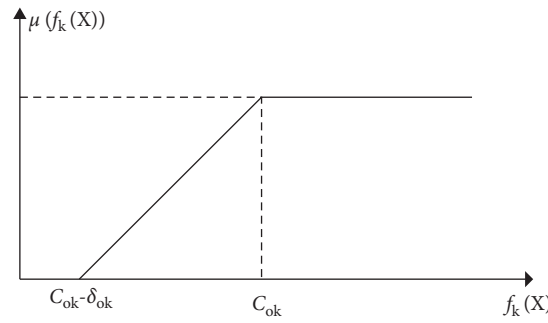

Figure 1: Membership function curve.

Step 1: the optimal solution of each single-objective function with constraints is identified based on the symmetrical manifold algorithm for chaotic optimization:

$$\begin{cases} \max f_i(X), & i = 1, 2, \cdots, p, \\ g_i(X) \le 0, & i = 1, 2, \cdots, m, \\ h_j(X) = 0, & j = 1, 2, \cdots, l. \end{cases} \tag{3}$$

Thus, the optimal solution for the above objective function with constraints is obtained.

Step 2: the value for each single target is extended to some extent; i.e., the determination of the value added.

Step 3: the objective function is fuzzy; i.e., the function for determining the membership of each objective function is expressed below:

$$\mu(f_k(X)), \quad k = 1, 2, \cdots, p. \tag{4}$$

Thus, it can be defined that the satisfaction to all membership functions is:

$$\lambda = \min\{\mu(f_i(X)), \mu(f_2(X)), \cdots, \mu(f_p(X))\}. \tag{5}$$

Step 4: c_{0k} and δ_{0k} are introduced into Eq. (2) to obtain p membership function expressions.

Step 5: based on the fuzzy set theory regarding the maximum/minimum law, the multi-objective issue is transformed into a single-objective nonlinear one by maximum satisfaction, with the mathematical model below.

$$\begin{cases} \max\lambda, \\ f_1(X) - \delta_{01}\lambda \ge c_{01} - \delta_{01}, \\ \cdots \\ f_k(X) - \delta_{01}\lambda \ge c_{0k} - \delta_{0k}, \\ \cdots \\ f_p(X) - \delta_{0p}\lambda \ge c_{0p} - \delta_{0p}, \\ 0 \le \lambda \le 1, \\ g_i(X) \le 0, \quad i = 1, 2, \cdots, m, \\ h_j(X) = 0, \quad j = 1, 2, \cdots, l. \end{cases} \tag{6}$$

Step 6: the single-objective fuzzy optimization model described above is solved based on the chaos

optimization symmetrical manifold algorithm to identify the optimal value for each objective function with satisfaction (90%) given.

The visual simulation system of mine engineering should have the following main functions:

(1) Integrated interface and data processing. Based on a database, combined with the actual situation of mine design, planning, and production, the system is to establish a mining engineering database. The database fully embodies the parameters related to the formation of mining projects, and can draw downhole projects correctly and flexibly based on the relevant data in the database. In addition, database management functions corresponding to the effective interface of general-purpose computer software systems such as AutoCAD systems are also required.

(2) The tunnels of the downhole mining project with the shape of the alley are divided into different types, the 3D solid modeling is carried out according to the parameters of each type, and the spatial position relationship is integrated into the overall downhole mining engineering system.

(3) The mapping of downhole mining project is divided into two parts: the exploitation system and the stope preparation mining cutoff system. They can be displayed separately in any designated space. Then, it rotates alternately in real time, and the construction staff can be observed from all angles through parallel movement and zooming. It can be drawn in full color in the graphic view to show the alley in three dimensions.

(4) It is planned to mine the pit engineering of the mine within an arbitrarily designated space, including the amount of ore and rock.

(5) Ore body display. The system can also perform 3D integration of mines and deposits. Engineers and technicians visually inspected the spatial relationship between alleys and deposits, and analyzed the rationality of the mining engineering composition.

The development environment that combines VC++ under Windows 2000/XP and chaos-optimized symmetric stream transmission algorithm [9, 10] is adopted for the visual simulation system of engineering within the mine. The chaotic optimization symmetric rheological algorithm is 100 or more graphics functions and hardware interfaces, which the developers can use to build 3D models and perform 3D real-time interaction. Chaos optimized symmetric flow pattern library has graphics functions, such as modeling, transformation, movement, complex frame buffer operations, light, color, shading, and texture surface processing.

Chaos optimization symmetric manifold algorithm instructions provide an interface between graphics software and hardware, and chaos optimization symmetric manifold algorithm subroutines is called to generate drawing instructions and data for hardware execution. The chaos-optimized symmetric flow transmission algorithm includes the following main steps in the process of operating graphics and finally drawing graphics on the screen:

(1) The geometric circles, points, and lines are used to construct object models and construct mathematical descriptions of objects.

(2) The object is chosen to place in an appropriate position in the 3D space to determine the optimal viewpoint for viewing the scene.

(3) Calculate the colors of all objects in the scene. The color of the object may come from the settings in the program, but if light and texture mapping are used in the scene, the final effect of the objects in the observed scene also depends on lighting and texture mapping.

(4) With regard to the object model, its mathematical description and color in the scene are converted through rasterization into pixels on the computer screen.

The chaotic optimization symmetric manifold algorithm can perform other operations, such as removing hidden surfaces. After the scene is rasterized, the scene can be drawn on the screen, and the pixels can be manipulated as needed. The basic operation process of the symmetric flow mode used for chaos optimization is to create an object model, determine the position of the viewpoint, calculate the color and lighting, and integrate the screen into one.

2.2. Application of Chaos Optimization Symmetrical Rheological Algorithm in Underground Mine Engineering

2.2.1. Entity Rendering. The chaotic optimization symmetric rheological algorithm has strong functions of creating and processing 3D graphics [11, 12], but the library functions are relatively limited, and only a dozen basic geometric graphics are provided. Quadric surface drawing functions are provided in the sublibrary, and most of the geometric centers are located at the origin (0,0,0). In this way, several sublibraries are drawn at any position, which can frequently change the system coordinates. Alternatively, graphical conversions can be performed in numerical matrix calculations. The latter is used to geometrically represent the corresponding position in this study. To effectively build a 3D visualization system for pit engineering of the mine, a large number of entity description function modules need to be made.

Chaotic Optimization Symmetrical Manifold shape is used for calculation function of program library, based on which arc surface cannot be generated directly. If the NURBS surface is not under proper control, the alley cannot be explained appropriately. Moreover, the scheme is complex with a low operating efficiency. In this study, a section is added to develop an arched alley consisting of two concentric cylinders with different radii and circular plates.

The key technology here is to define additional clipping planes to eliminate targets that are irrelevant to the scene. The additional plane clipping function is voidgl ClipPlane (Glonumpline, ConstGrouble * equation), which defines the

additional clipping plane. Here, the parameter equation refers to an array with four coefficient values. The four coefficients are the A, B, C, and D values of the clipping plane $Ax + By + Cz + D = 0$. The cross section can be determined based on these four coefficients. The parameter plne is GL CLIP. LANEi assigns ($i = 0, 1$) as the number of the clipping plane. Before calling the additional clipping function, the clipping plane currently defined by glEnbale.CLIP_pLANEi must be activated. If the additional section is not activated, go to the glDiable (GL) tab, and CLIP_pLANEi will close the corresponding additional clipping function.

The program modules for drawing arc-shaped roadways are:

```
GLdoubleequ[4] = {1,0,0,1 * (t_ArcData.m—r-t_
ArcData. m_width/2) * cos (t_ArcData.
PI/180)/10); //Set the cutting plane
glPJJshMatrix();
glTranslated((t—ArcData.m_ox-xStartCord)/10,
m_oz-zStartCord + t_ArcData. mhigh)/10,
(t_ArcData. m_oy-yStartCord)/10);//Translate to the
center of circle
glRotatef(1 * (atan2(t—ArcData.mpy-t—ArcData.
m_oy, t_ArcData. mpx-t_ArcData.
M_ox)/PI * 180), 0.0,1.0,0.0); //counter revolution
glClipPlane(GL_CLIP—PLANEO,equ);
GlEnable(GL_CLIP_PLANEO); //activate the cutting
function, increase the clipping plane
g1Rotatef(90, l.0,0.0,0.0); //90° around x
quadObj = glu.NewQuadric();
gluQuadricDrawStyle(quadObj, GLU_FILL);
gluQuadricOrientation(quadObj, GLU_OUTSIDE);
//The normal direction is outward
gluQuadricNormals(quadObj, GLU_SMOOTH);
gluCylinder(quadObj,(t_ArcData.m—r + t_ArcData.
m_width/2)/10,
(t_ArcData.m_r + t_ArcData.m_width/2)/10,
t_ArcData. m_high/10,30,30); II draw outer cylinder
glPushMatrix();
Gl Translate f(0,0, t_ArcData. m_height/100)//parallel
translate to the horizontal bottom plate
Disk(quadObj,(t_ArcData. m_r-t_ArcData.
m_r + t_ArcData. m_width/2) 110, 30, (2)//depict the
glPopMatrix of the bottom disc
();
gluQuadricOrientation(quadObj, GLU_INSIDE);
//The normal direction is inward
gluCylinder(quadObj,(t_ArcData. m_r-t_ArcData.
m_width/2)/10, t_ArcData. m_//Draw the inner cylinder
Disk(quadObj,(t_ArcData. m_r-t_ArcData.
m_r + t_ArcData. m_width/2) 110, 30, (2)//Draw the
top of the mountain
glu. DeleteQuadric(quadObj);
glDisable(GL_CLIP_pLANE0);
//Close the cropping function glPopMatrix();
```

2.2.2. Projective Transformation. Projective transformation is an essential technique for transforming graphics to identify a frustum and intercept the excess beyond the FOV. The final image is only the relevant part of the frustum [13, 14]. The chaotic optimization symmetric rheological algorithm provides two projection methods: orthographic projection and perspective projection. The field of view of the orthographic projection is a rectangular parallel pipe. Orthographic projection is characterized by the constant object size after projection however far the object is from the viewpoint. This projection is usually suitable for drawing and computer-aided design of pit engineering in the mine. In these application areas, the size and mutual angle of the projected objects do not change, so the proportions of the objects during construction are correct.

In perspective projection, the larger the projection of approach point is, with the projection from viewpoint getting smaller, the projection reaching climax will disappear and become a vanishing point. The upper and lower cervical vertebrae are cut out from frustum of perspective projection, that is, the frustum of a pyramid; the projection is applied to areas where animations, visual simulations, and other realistic images of wings are requested. In the visualization system of mine downhole engineering, this system uses orthographic projection to intuitively analyze the rationality of the mine downhole engineering layout to show the spatial position relationship between the projects. After the projection transformation, there will be no change in the proportional relationship between alleys.

Based on the Chaotic Optimization Symmetrical Manifold algorithm, there are various light models such as the model for radiation, ambient, diffused, and specular light [15]. Among them, radiation is directly emitted from the object, which is not subject to influence by light sources. Ambient light is scattered several times from the light source in the environment; in this way, the light may seem to have come from all directions and cannot be determined. Diffused light comes from a certain direction; when it is perpendicular to the object, it looks brighter than when it is tilted after reaching the object, and it is uniformly distributed in all directions. Likewise, specular light comes from a specific direction and is distributed in other directions.

The light source has a series of characteristics. For example, color, position, and direction. If different characteristic values are selected, the effect of the corresponding light source on the object will be different. The function that defines the characteristics of the light source is flight ∗ : void gl Light {if}[v](Gronumlight, Groumpname, TYPE param). Here, the first parameter light specifies the number of the light sources created, the second parameter pname specifies the characteristics of light source, and the last parameter sets the characteristic value of corresponding light source.

The light model is established to fully cover the graphic image generated in complicated computation on normal objects, light sources, and materials. The lighting model is initiated by command (glEnbale. LIGHTING), and the light is turned off by gDiscable (GL_LIGHTING).

In the calculation, the vector indicates the direction amount several countries strictly. The angle of light reaching an object for OpenGL should be calculated based on the normal vector to generate 3D images, and the normal vector of the object should be defined accordingly.

The normal vector is defined by 2 function in the chaotic optimization symmetric manifold algorithm. The first means that according to the function, three components nxnz of the normal vector are obtained. The second means to pointer v with three elements is defined. Since no function for corona calculation is provided based on the chaotic optimization symmetric rheological algorithm, the corresponding program should be created by the developer. Based on practical data, the normal vector algorithm proposed in this study is proved to be accurate and effective.

The following features are observed in the development process.

(1) For the sake of more convenient development and application, the system is designed based on the modular concept. A 3D dynamic visualization system and related modules of equipment are established for pit engineering. This modular structure can be used to construct the downhole workers in different mines. The system requirement can be determined by 3D dynamic visual simulation.

(2) In CAD engineering drawing of mine production systems such as the mine development and mining planning in practice, it is possible to adapt the whole logistics flow of the simulation system model to the practical one by structural configuration and simulation system establishment.

(3) The setting and input of analog parameters are very convenient. Due to the powerful interaction of the WITNESS simulation software, it can interact with the EXCEL software of the OFFICE software package. The XLReadArray function and XLWriteArray function can be used to read different types of parameter variables in WITNESS, such as integer, real, name, and string, into the WITNESS system or to write to EXCEL in this way; outside the WITNESS simulation software simulation model system, parameters can be changed and the simulation data can be displayed on EXCEL in real time. Hence, the input parameters of the system parameters can be set based on the specific requirements and goals of the mine, and the parameter control in EXCEL can be used to intervene in the system simulation, without operating the simulation software to reduce the difficulty of operation.

3. Example and Result Analysis

In this system, a simulation model for in-pit visual production system of the mine is first established as the case may be and verified, and then simulation is conducted during in-pit production process. Moreover, real-time analysis is performed at each operating stage of the mine flow system. The development logic for the 3D dynamic visual simulation system of downhole engineering in mines is described as follows:

(1) Information on the mine production system in the specific mine is collected, including parameters related to the tunneling system, the logistics process, productivity, technical parameters, and equipment capacities in the production system of coal mining, ventilation, transportation, and drainage.

(2) Statistical analysis combined with the collected data on the 3D dynamic visual simulation system of downhole mine engineering.

(3) Analysis of influencing factors in mine production. The boundary of the mine logistics system is defined, and the subsystems are further classified by the functions of the logistics process.

(4) Determination of the statistical rules and parameters in each part of the mining system according to the results of field investigation and statistical analysis.

(5) Identification of the correlation between various subsystems in mine production based on the mine layout and production systems of a built mine. The integration capacity of mine production and logistics system equipment is determined, and a fully visualized 3D dynamic visual simulation system for downhole mine engineering is constructed.

(6) Conversion of 3D dynamic visual simulation system model for downhole mine engineering into computer simulation model appropriately by simulation software WITNESS.

(7) Verification of the reliability of the simulation model. Statistical analysis is conducted on the simulation results after random influencing factors are removed to identify the unreasonable factors therein.

(8) Model improvement and adaptation to the practical mine production system.

(9) Simulation of the mine logistics system based on practical mine production. Based on the simulation results, the mine logistics system is optimized and appropriately combined. The improvement scheme is applied to the practice of mine production and evaluated by comparing the improved demonstration operation to the actual production.

In the development of the 3D dynamic visual simulation system, the key problems are described below.

(1) Firstly, the real mine production system data of the specific mine, including the parameters of the tunneling system, logistics process, production system (coal mining, excavation, ventilation, transportation, drainage) capacity, and technical parameters and capacities of relevant equipment, are collected.

(2) The drawings for engineering such as mine development engineering drawings (Figure 2), mining

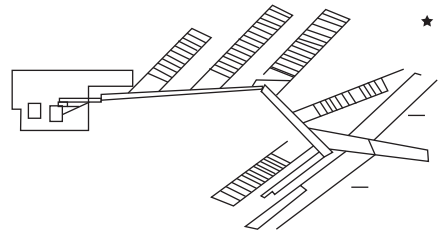

Figure 2: Mine development project map (partial).

Table 1: Structure of 3D dynamic visual simulation system modules.

S/N	Name of the module	Content of the module	Role of the module
1	Excavation equipment	Shearers, supports, roadheaders, etc.	Equipment selection and layout deployment
2	Transportation equipment	Mine cars, belt conveyors, transfer conveyers, mine truck dumpers, scraper conveyors, etc.	
3	Lifting equipment	Main and auxiliary shaft hoists, cages, mini hoists, etc.	
4	Ventilation equipment	Fans, dampers, air ducts, etc.	
5	Drainage equipment	Water pumps, pipelines, water ditches, and water chambers	
6	Downhole personnel	Coal mining, tunneling and supporting personnel, maintenance personnel, management personnel, et al.	Management of personnel
7	Roadway	Horizontal main alley, downhole parking lot, main haulage roadway, transportation up/down the hill, rock crosscut, etc.	3D dynamic visualization of downhole engineering
8	Downhole chamber	Coal bunkers, gangue bunkers, etc.	Deployment of system layout
9	Main and auxiliary shafts	Main shafts, auxiliary shafts, air shafts	
10	Surface coal	Merged mining, conventional mining	Method selection for coal mining
11	Surface tunneling	Comprehensive tunneling, general tunneling, etc.	Method selection for tunneling
11	CAD	CAD system, CAD database	Data import and drawing by using CAD
12	JMP analysis	Analysis indexes for system reliability, etc.	Analysis of system reliability
13	Auxiliary feature	System maintenance and other modules	Addition of other auxiliary system features

engineering drawings, etc., ares imported into the WITNESS system. The prebuilt system modules (Table 1) are imported according to the practical 3D dynamic visualization of downhole engineering (see Figure 3), and a simulation system model for in-pit visualization production is established.

The 3D dynamic visual simulation of downhole engineering is based on the established goals and empirical data of the system, and the visual simulation of the system that has not been designed is used as the basis for the design of the actual system. Secondly, mainly combined with practical mine production systems, 3D dynamic visualization system for practical downhole engineering (coal collection, excavation, drainage and ventilation) in the pit can be simulated simultaneously after on-site investigation and acquisition of relevant logistics data. Based on the simulation statistical analysis of the downhole engineering 3D dynamic visualization system and the system and equipment reliability analysis results, further simulation analysis was carried out for the evaluation and prediction analysis of mine production capacity. According to the forecast of mine production capacity, the various subsystems (production, transportation, ventilation, drainage, etc.) of the production system in the pit are comprehensively considered. The production capacity of the mine plan is comprehensively established to provide a basis for making decisions on the mine production plan based on the mine operation capacity.

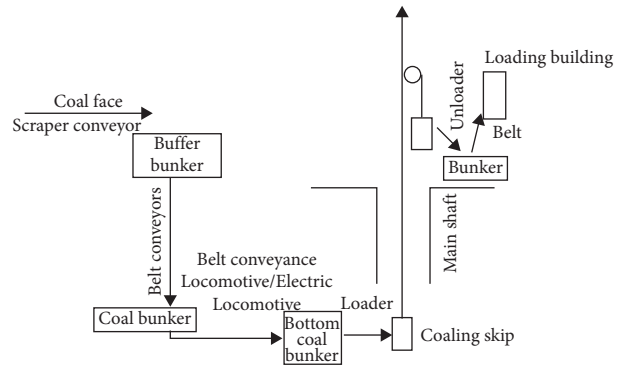

Figure 3: Process flow of 3D dynamic visualization of downhole mine engineering.

Based on meeting the planned production capacity of the mine and the continuity of mining and production,

simulation analysis is carried out according to the actual mining process of the mine, and the situation of continuous mining under the conditions of different coal mining footage, number of heading ends and footage is analyzed to ensure a balanced mining plan and to provide support for the continuous mining plan of the mine. In the system simulation, economic indicators such as the actual statistical analysis of the mine and the work cost of the survey agency are set as simulation parameters. During the set simulation operation cycle, the logistics situation of the production system in the mine and the influencing factors that restrict the normal production in the mine are comprehensively analyzed through simulation and forecast of logistics cost of in-pit production and comparison with simulation result of actual in-pit logistics cost, thereby the plans and measures needed to improve the normal production of the mine is proposed. The predicted cost for 3D dynamic visualization of downhole mine engineering can be obtained. The in-pit logistics is reasonably planned, and the increase of logistics cost is realized. A basis for decision-making is provided.

4. Conclusion

Chaotic optimization symmetrical manifold algorithm technology can be used to visually simulate downhole mining projects, real-time rotation, translation, zooming in and out in alleys, with fast running speed, and the engineering images in the mine pit are realistic, which makes people feel real. The design and planning database obtained by the computer-aided design system is used to generate 3D moving images of downhole mine projects through further research, and then virtual roaming in the alley is realized to provide a means for engineers and technicians to intuitively analyze and optimize the configuration of downhole mining projects.

Data Availability

The data used to support the findings of this study are available from the corresponding author upon request.

Conflicts of Interest

The authors declare that they have no conflicts of interest.

Acknowledgments

This research study was sponsored by Liaoning Revitalization Talents Program, project no. XLYC1807219.

References

[1] W. Yang, Z. Ai, X. Zhang, R. Gou, and X. Chang, "Nonlinear three-dimensional dynamics of a marine viscoelastic riser subjected to uniform flow," *Ocean Engineering*, vol. 149, pp. 38–52, 2018.

[2] I. D. Moore and F. Guan, "3D dynamic response of lined tunnels due to incident seismic waves," *Earthquake Engineering & Structural Dynamics*, vol. 25, no. 4, pp. 357–369, 2015.

[3] Y. Liu, Z. Wu, Q. Yang, and K. Leng, "Dynamic stability evaluation of underground tunnels based on deformation reinforcement theory," *Advances in Engineering Software*, vol. 124, pp. 97–108, 2018.

[4] D. Conroy and O. K. Matar, "Dynamics and stability of 3D ferrofluid films in a magnetic field," *Journal of Engineering Mathematics*, vol. 107, no. 1, pp. 1–16, 2017.

[5] Y. Liang and Q. Liu, "Early warning and real-time control of construction safety risk of underground engineering based on building information modeling and internet of things," *Neural Computing & Applications*, vol. 34, no. 5, pp. 3433–3442, 2021.

[6] S. A. Ghoreishi-Madiseh, A. P. Sasmito, F. P. Hassani, and L. Amiri, "Performance evaluation of large scale rock-pit seasonal thermal energy storage for application in underground mine ventilation," *Applied Energy*, vol. 185, no. 2, pp. 1940–1947, 2017.

[7] Z. Z. Liu, P. Cao, H. Lin, J. J. Meng, and Y. X. Wang, "Three-dimensional upper bound limit analysis of underground cavities using nonlinear Baker failure criterion," *Transactions of Nonferrous Metals Society of China*, vol. 30, no. 7, pp. 1916–1927, 2020.

[8] P. Shan and W. Sun, "Analysis of thermal effect around an underground storage cavern with a combined 3D indirect boundary element method," *Engineering Analysis with Boundary Elements*, vol. 95, pp. 255–265, 2018.

[9] D. S. S. SandanayakeSandanayake, E. Topal, and M. W. Ali AsadAli Asad, "A heuristic approach to optimal design of an underground mine stope layout," *Applied Soft Computing*, vol. 30, pp. 595–603, 2015.

[10] J. Menéndez, J. Loredo, M. GaldoGaldo, and J. M. Fernández-OroFernández-Oro, "Energy storage in underground coal mines in nw Spain: assessment of an underground lower water reservoir and preliminary energy balance," *Renewable Energy*, vol. 134, pp. 1381–1391, 2019.

[11] V. Y. A. Chirkunov and Y. L. Skolubovich, "Nonlinear three-dimensional diffusion models of porous medium in the presence of non-stationary source or absorption and some exact solutions," *International Journal of Non-Linear Mechanics*, vol. 106, pp. 29–37, 2018.

[12] X. D. Song, H. Y. WuWu, F. Liu et al., "Three-Dimensional mapping of organic carbon using piecewise depth functions in the red soil critical zone observatory," *Soil Science Society of America Journal*, vol. 83, no. 3, pp. 687–696, 2019.

[13] A. Jahanbakhshzadeh, M. Aubertin, and L. Li, "3D stress state in inclined backfilled stopes obtained from numerical simulations and new closed-form solution," *Canadian Geotechnical Journal*, vol. 55, no. 6, pp. 810–828, 2018.

[14] A. Kapahi and H. S. Udaykumar, "Three-dimensional simulations of dynamics of void collapse in energetic materials," *Shock Waves*, vol. 25, no. 2, pp. 177–187, 2015.

[15] G. Prerna and S. David, "3D multicomponent vesicles: dynamics & influence of material properties," *Soft Matter*, vol. 14, no. 1, pp. 1–7, 2018.